International Immunopharmacology 76 (2019) 105874

Contents lists available at ScienceDirect

International Immunopharmacology

journal homepage: www.elsevier.com/locate/intimp

The small molecule macrophage migration inhibitory factor antagonist MIF098, inhibits pulmonary hypertension associated with murine SLE

Huijing Huang[a], Dandan Chen[a], Jun Pu[b], Ancai Yuan[b], Qiong Fu[a], Jia Li[a], Lin Leng[c], Richard Bucala[c], Shuang Ye[d,*], Liangjing Lu[a,**]

[a] Department of Rheumatology, Ren Ji Hospital, Shanghai Jiaotong University School of Medicine, Shanghai, China
[b] Department of Cardiology, Ren Ji Hospital, Shanghai Jiaotong University School of Medicine, Shanghai, China
[c] Department of Medicine, Yale University School of Medicine, New Haven, CT, USA
[d] Department of Rheumatology, Ren Ji Hospital South Campus, Shanghai Jiaotong University School of Medicine, Shanghai, China

ARTICLE INFO

Keywords:
Systemic lupus erythematosus
Pulmonary arterial hypertension
Macrophage migration inhibitory factor

ABSTRACT

Pulmonary arterial hypertension (PAH) is a severe complication of systemic lupus erythematosus (SLE), with unclear etiopathogenesis. We evaluated the role of macrophage migration inhibitory factor (MIF), which has been implicated in idiopathic pulmonary hypertension (PH), in SLE-associated PAH. Circulating MIF was measured in SLE patients, SLE-PAH patients, and healthy donors. *In situ* pulmonary artery MIF protein expression was determined in spontaneous SLE mice (MRL/*lpr*) and hypoxia-induced C57BL/6J mice. Daily MIF098 was administered to C57BL/6J mice, and these mice were maintained in a hypoxic chamber for 4 weeks. The right ventricular systolic pressure (RVSP) and pathological characteristics of the pulmonary artery (PA), such as hyperproliferation, muscularization, and fibrosis were then measured in each group of mice. Data were also obtained *in vitro* using pulmonary smooth muscle cells (PASMC) challenged with platelet-derived growth factor (PDGF)-BB or 1% O_2 hypoxia. As a result, circulating MIF was elevated in SLE-PAH patients compared with SLE patients or healthy donors. Higher RVSP SLE mice produced more MIF protein than lower RVSP SLE mice in the pulmonary artery. MIF098 decreased RVSP and inhibited distal pulmonary artery hyperproliferation, muscularization, and collagen deposition in hypoxia challenged mice. In addition, MIF098 inhibited PASMC proliferation and migration by regulating mitogen-activated protein kinase/extracellular signal-regulated kinase 1/2 (MAPK/ERK1/2) signal- and cell-cycle-related proteins. MIF098 also reduced collagen synthesis by inhibiting the TGFβ1/Smad2/Smad3 pathway in cell-based experiments. In conclusion, MIF may serve as a biomarker and a therapeutic target of SLE-associated PAH. Pharmacologic MIF antagonism may be an effective means to ameliorate SLE-PAH.

1. Introduction

Systemic lupus erythematosus (SLE) is an autoimmune disease characterized by aberrant host innate and adaptive immune response and a wide spectrum of disease manifestations [1]. Among them, pulmonary arterial hypertension (PAH) is one of the most severe complications and the third leading cause of mortality in SLE patients [2,3]. PAH can occur at any time during the course of SLE, and once PAH develops, outcomes are poorer than in patients with idiopathic PAH (iPAH) [4–6]. A better understanding of SLE-PAH may lead to more effective prevention and treatment of this severe complication of SLE.

PAH is a clinical condition characterized by the presence of pre-capillary pulmonary hypertension, which is defined as a high mean pulmonary artery pressure (≥25 mmHg) at rest, confirmed by right heart catheterization (RHC) and in the presence of normal pulmonary capillary wedge pressure (PCWP ≤15 mmHg) and increased pulmonary vascular resistance (PVR > 3 Wood units) [7,8]. The most important pathological characteristics are abnormal vascular remodeling, excessive pulmonary vasoconstriction, *in situ* thrombosis, and inflammatory cell infiltration [9]. Various autoantibodies, including antinuclear antibodies, anti-phospholipid antibodies, and anti-endothelial cell antibodies, as well as different immune mediators can be detected in the pulmonary arteries in SLE-PAH patients [10]. Specific drugs are lacking, and current therapeutic approaches for SLE-PAH patients

* Correspondence to: S. Ye, Department of Rheumatology, Ren Ji Hospital South Campus, Shanghai Jiaotong University School of Medicine, Shanghai 200127, China.
** Correspondence to: L. Lu, Department of Rheumatology, Ren Ji Hospital, Shanghai Jiaotong University School of Medicine, Shanghai 200127, China.
E-mail addresses: ye_shuang2000@163.com (S. Ye), lu_liangjing@163.com (L. Lu).

https://doi.org/10.1016/j.intimp.2019.105874
Received 17 June 2019; Received in revised form 31 August 2019; Accepted 1 September 2019
Available online 06 September 2019

follow the treatment of iPAH, such as prostacyclin analogs, phosphodiesterase (PDE)-5 inhibitors, and endothelin receptor antagonists (ERA) [11,12]. These interventions are insufficient to suppress the progression of vascular remodeling, however, which is the key pathological feature of PAH.

Macrophage migration inhibitory factor (MIF) is an upstream inflammatory cytokine released from numerous cell types, such as macrophages, T-cells, and dendritic cells [13,14], as well as by pulmonary epithelium [15]. MIF activates its cognate receptor CD74, leading to the activation of the mitogen-activated protein kinase/extracellular signal-regulated kinase 1/2 (MAPK/ERK1/2), AKT, and nuclear factor κB (NFκB) pathways, and downstream proliferation and enhanced survival [16,17]. MIF promotes cell cycle progression and suppresses P53-mediated cell-cycle arrest [16,18]. MIF plays a deleterious role in various inflammatory disorders, such as rheumatoid arthritis, systemic sclerosis, including systemic sclerosis PAH, and sepsis [19–22]. Elevated MIF plasma concentrations are detected in PAH patients, and PAH pulmonary arterial cells, including endothelial cells and smooth muscle cells, express a high level of MIF and CD74 [23–25]. MIF gene deficiency or treatment with the prototypic MIF antagonist ISO-1 has been shown to decrease right ventricular systolic pressure and reduce the progression of pulmonary artery remodeling [24,26]. The potential contribution of MIF to the PAH which occurs in SLE, where MIF is overexpressed, has not been studied. In this study, we assessed MIF levels in SLE-PAH patients and SLE-PAH mice. In addition, we explored whether MIF antagonist 3-(3-hydroxybenzyl)-5-methylbenzooxazol-2-one, designated MIF098, could ameliorate the pathological progression of PAH.

The chemical structure of MIF098 ($C_{15}H_{13}NO_3$) is shown in Fig. 1. In a study of Shin MS et al., MIF098, which blocks MIF binding to its cognate receptor CD74, suppressed NLRP3 upregulation, a rate-limiting step in activating the NLRP3 inflammasome, as well as caspase-1 activation and downstream interleukin (IL)-1β production in snRNP immune complex-stimulated human monocytes [27]. MIF098 also has been reported to inhibit the phosphorylation of ERK1/2 by preventing MIF-CD74 interaction in synovial fibroblasts [28,29]. We therefore investigated whether pharmacologic MIF antagonism with MIF098 could ameliorate PAH in a relevant mouse model of SLE.

2. Materials and methods

2.1. Study population

Sera from 3 cohorts of subjects were studied. The patients with SLE were enrolled if they conformed to the 1997 revised American College of Rheumatology (ACR) criteria [30]. Age- and sex-matched SLE-PAH patients were collected in accordance with both SLE and PAH criteria. PAH was diagnosed by right heart catheterization with a mean pulmonary arterial pressure (mPAP) ≥25 mmHg, plus a pulmonary capillary wedge pressure (PCWP) ≤15 mmHg, and pulmonary vascular resistance (PVR) > 3 Woods units. Ten healthy donors were also enrolled in this study. The clinical characteristics of the patients in the 3 groups is shown in Table 1. The study was approved by the Ethics Review Board at Ren Ji Hospital, Shanghai Jiaotong University (No. 2017201).

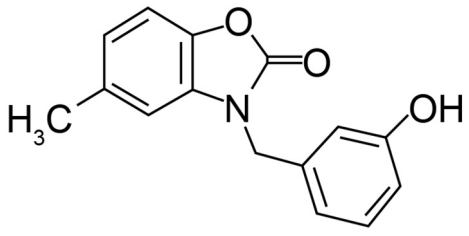

Fig. 1. The chemical structure of MIF098.

Table 1
Characteristics of the study groups.

Parameters	Health (n = 10)	SLE (n = 15)	SLE-PAH (n = 15)
Age, years	43.8 ± 8.8	41.0 ± 12.7	37.9 ± 9.5
Female, n (%)	7(70)	14(93.3)	13(86.7)
SLE duration, months	–	92.7 ± 99.6	102.3 ± 80.2
SLEDAI	–	5.2 ± 4.7	4.5 ± 2.6
PAH duration, months	–	–	30.5 ± 27.2
WHO functional class, n (%)			
I	–	–	2(13.3)
II	–	–	5(33.3)
III	–	–	6(40)
IV	–	–	2(13.3)
PASP, mmHg	–	–	74.0 ± 6.5
PADP, mmHg	–	–	69.5 ± 16.6
mPAP, mmHg	–	–	35.9 ± 6.5
PCWP, mmHg	–	–	6.7 ± 3.4
PVR, Wood units	–	–	10.3 ± 3.9
BNP, pg/ml	–	–	693.4 ± 285.2
LVEF, %	–	–	66.4 ± 7.7
CO, liter/min	–	–	3.5 ± 1.4

SLEDAI = Systemic Lupus Erythematosus Disease Activity Index; WHO = World Health Organization; PASP = pulmonary artery systolic pressure; PADP = pulmonary artery diastolic pressure; mPAP = mean pulmonary artery pressure; PCWP = pulmonary capillary wedge pressure; PVR = pulmonary vascular resistance; BNP = brain natriuretic peptide; LVEF = left ventricular ejection fraction; CO = cardiac output.

2.2. Animals

Female MRL/*Fas*^{lpr} (*lpr*) mice (BALB/c background) and 25 male C57BL/6J mice were purchased from Shanghai SLAC Laboratory Animal Co Ltd. (Shanghai, China). All animals were maintained under the Specific Pathogen-Free (SPF) conditions with a 12 h light/12 h dark cycle, a temperature of 24–25 °C, and *ad libitum* access to standard chow and water at the SLAC Experimental Animal Center. All of the aspects of animal care and experimentation performed in this study were approved by the Animal Research Committee at Renji Hospital, Shanghai Jiaotong University.

2.3. Hypoxic mouse model of PAH and experimental protocols

To induce pulmonary arterial hypertension, male C57BL/6J mice were exposed to hypoxia in a chamber (XBS-03, Aipu, Hangzhou, China) for 4 weeks. In the hypoxic chamber, oxygen was tightly regulated, nitrogen was automatically introduced to maintain the proper fraction of inspired oxygen (FiO_2, 10%). Age- and sex-matched littermates were exposed to normoxia (room air, 21% O_2) and served as controls. In the treatment groups, the MIF antagonist MIF098 (4 mg/ml, dissolved in 10% dimethyl sulfoxide (DMSO)) was injected intraperitoneally into hypoxic mice at a dosage of 40 mg/kg once a day started at the day they received hypoxia exposure until the exposure ended. An equal number of C57BL/6J mice were treated with 10% DMSO daily in hypoxic conditions as a PAH model group. Mice kept in normoxic conditions served as negative controls. The chamber was open < 20 min every day for intraperitoneal injection or drug or vehicle.

2.4. Measurement of RV pressure and tissue collection

Four weeks after hypoxia exposure, mice were used for RVSP measurement. Mice were anesthetized by an intraperitoneal injection of 4% chloral hydrate at a dosage of 0.1 ml/10 g body-weight. The right internal jugular vein was exposed after bluntly dissecting the neck skin of the animal. Then, a 1.4F Millar catheter (SPR-671, Mikro-Tip, Houston, USA) was inserted into the right ventricle and RV pressure was recorded. After data collection, mice were euthanized by cervical

dislocation. Lung tissues were removed and fixed in 4% paraformaldehyde for H&E staining and immunohistochemical staining. The ratio of the weight of right ventricle to that of the left ventricle (LV) plus septum (S) was used to assess right ventricle (RV) hypertrophy.

2.5. Enzyme-linked immunosorbent assay (ELISA)

Human sera were 1:100 diluted with distilled water before the measurement. MIF concentrations were measured with the Human MIF ELISA Kit (Thermo Scientific, USA) according to the manufacturer's instructions. The plate was read with a microplate reader (Thermo Scientific, USA) at the absorbance of 450 nm wavelength. Data were analyzed with GraphPad Prism Version 6.00 (GraphPad Software, La Jolla, CA, USA).

2.6. Immunohistochemistry (IHC)

Paraffin lung tissues were cut into 5-μm-thick sections. After deparaffinization and hydration, sections were incubated with primary antibodies against α-smooth muscle actin (α-SMA, ab7817, Abcam, USA), MIF (ab7207, Abcam, USA), or Ki67 (ab16667, Abcam, USA) at appropriate concentrations. Diluted biotinylated secondary antibodies were added, and sections were incubated at room temperature for 30 min. Then sections were incubated in the Streptavidin-Biotin Complex (SABC, BOSTER, Wuhan, China) for 20 min. Finally, sections were treated with diaminobenzidine (DAB) substrate solution until the desired color intensity was achieved.

2.7. Cell culture

Mouse pulmonary artery smooth muscle cells (mPASMCs) were purchased from the American Type Culture Collection (ATCC). Cells were cultured in Dulbecco's modified Eagle's medium (DMEM) containing 10% fetal bovine serum (FBS) and 100 mg/ml of penicillin and 100 IU/ml of streptomycin and incubated at 37 °C in a humidified atmosphere (5% CO_2 in air). Cells at passages 3–5 were used for experiments. Before reagents were added to the plates, mPASMCs were starved for 24 h by incubating in serum-free DMEM, then culture was replaced in DMEM containing 1% FBS for further stimulation.

2.8. Cell counting kit 8 (CCK8) cell proliferation assay

mPASMCs were seeded in 96-well plates at a density of 3000 cells per well. After 24 h of starvation, cells were stimulated with 20 ng/ml of platelet-derived growth factor-BB (PDGF-BB, Pepro Tech, Rocky Hill, USA) or exposed to 1% O_2, and various concentrations (0, 10 nM, 100 nM, 1 μM, 10 μM) of MIF098 were used as treatments for 48 h. Culture was removed, and DMEM containing 10% Cell Counting Kit-8 reagent (Dojindo, Kumamoto, Japan) was added into each well. The absorbance at 450 nm was measured with a microplate reader (Thermo Scientific, USA) after 2 h of incubation at 37 °C in the dark. Each group included 6 wells, and means and standard deviations were calculated after elimination of any outlying values (> 2 SDs).

2.9. EdU staining

The Cell-Light™ EdU Apollo®488 *In Vitro* Imaging Kit (Ribobio, Guangzhou, China) was used to detect cell proliferation. After treatments, cells were incubated with EdU (5-ethynyl-2′-deoxyuridine) for 2 h at 37 °C. Then, cells were fixed with 4% paraformaldehyde and permeabilized with 0.5% Triton X-100 for 20 min. After washing 3 times with phosphate-buffered saline (PBS), cells were incubated with 1× Click-iT reaction cocktails for 1 h at room temperature. PASMC nuclei were stained by Hoechst 33342 for cell enumeration. EdU-positive cells were visualized with an inverted fluorescence microscope (Nikon, Japan) at a wavelength of 488 nm. Three randomly selected views from each sample image were used to calculate the relative EdU-positive ratio for quantification of the PASMC proliferative rate.

2.10. Cell migration assay

Cell migratory ability *in vitro* was evaluated by wound-healing assay and a Transwell system. A scratch was made by p10 pipette tip on confluent monolayer cells. After 24 h of treatment, photos were taken, and the decreased width of the scratch was measured. The Transwell migration system contained 12-μm polycarbonate membrane hanging cell culture inserts (Costar, USA) in 24-well culture plates. Untreated mPASMCs were starved for 24 h, then cells were digested and transferred into the upper inserts of plates at a number of 5×10^4 cells per well. The 24-well plate was incubated for 12 h, and cells on the membranes of the Transwell inserts were fixed with 4% paraformaldehyde. After detaching non-migrated cells from the upper surface of inserts, cells that migrated to the lower surface were stained with 0.3% crystal violet (Beyotime, China) for 30 min. Cells in 5 random fields were counted under an optical microscope (Nikon, Japan).

2.11. Immunofluorescence

PASMCs were seeded on cover glasses in a 6-well plate. After 48 h of incubation with stimuli, cells were fixed with 4% paraformaldehyde for 20 min. Then, cells were treated with 0.3% Triton X-100 and 5% normal goat serum in PBS for 1 h at room temperature. Diluted Ki67 (1:100 dilution, ab16667, Abcam, UK) primary antibody was added on the glass, and cells were incubated in a humidified box at 4 °C overnight. Cells were incubated with the recommended dilution of the secondary antibody (Alexa Fluor® 488 Conjugate, Cell Signaling Technology, 8494S, USA) at room temperature for 1 h. DAPI was used to stain nucleus for 5 min. Photos were taken under a fluorescence microscope (Nikon, Tokyo, Japan).

2.12. Picrosirius red staining and Masson trichrome staining

Picrosirius Red staining and Masson trichrome staining was used to determine the content of collagen in tissues. For Picrosirius Red staining, paraffin sections were de-waxed, hydrated, and stained with hematoxylin and Picrosirius Red. Sections were observed under an optical microscope (Nikon, Japan). The protocol of Masson trichrome staining was described previously [31]. Images were analyzed using Image-Pro Plus software (National Institutes of Health, USA).

2.13. Immunoblotting

PASMC lysates were extracted by ice-cold radioimmunoprecipitation assay (RIPA) buffer (Beyotime, China) containing 1% phenylmethanesulfonyl fluoride (Beyotime, China). Protein samples were subjected to electrophoresis in sodium dodecyl sulfate polyacrylamide gel electrophoresis (SDS-PAGE), then transferred to polyvinylidene difluoride membranes (Millipore, USA). After blocking in 5% skim milk for 60 min at room temperature, membranes were incubated with the primary antibodies against MIF (1:2000 dilution, ab7207, Abcam, UK), P53 (1:1000 dilution, ab131442, Abcam, UK), P21 (1:1000 dilution, ab188224, Abcam, UK), Cyclin D1 (1:1000 dilution, ab134175, Abcam, UK), CDK4 (1:1000 dilution, ab108357, Abcam, UK), CDK6 (1:1000 dilution, ab124821, Abcam, UK), p-ERK1/2 (1:1000 dilution, Cell Signaling Technology, 4370, USA), ERK1/2 (1:1000 dilution, Cell Signaling Technology, 4695, USA), Collagen I (1:1000 dilution, ab34710, Abcam, UK), Collagen II (1:1000 dilution, ab34712, Abcam, UK), Fibronectin (1:1000 dilution, ab2413, Abcam, UK), p-Smad2 (1:1000 dilution, ab53100, Abcam, UK), p-Smad3 (1:1000 dilution, ab52903, Abcam, UK), Smad2/3 (1:1000 dilution, Santa-Cruz, sc-133,098, USA) or β-actin (1:1000 dilution, Cell Signaling Technology, 3000 T, USA) at 4 °C overnight. Membranes were

subsequently incubated with appropriate horseradish peroxidase-conjugated secondary antibodies (1:5000 dilution, Cell Signaling Technology, 7074 or 7076, USA) for 1 h at room temperature. Protein bands were visualized using enhanced chemiluminescence (Tanon 5200, China).

2.14. SiRNA transfection

mPASMCs were transfected with small-interfering RNA (siRNA) according to the manufacturer's instructions (Ribobio, China) after cells reached 30–40% confluence. Further treatment was performed after mPASMCs had been transfected with siRNA for 48 h.

2.15. Data analysis

All values were expressed as means ± standard error of mean. Group comparisons were evaluated by unpaired Student's *t*-test. Pearson's correlation analyses were performed when indicated. P values < 0.05 or less were considered statistically significant. All analysis was performed using Graphpad Prism 6.0 software (Graphpad Software, Inc., La Jolla, CA, USA) and SPSS software version 20.0 (SPSS, Inc., USA).

3. Results

3.1. MIF levels are increased in sera of SLE-PAH patients, as well as in high-RVSP SLE mice and in the pulmonary arteries of hypoxia-induced mice

We examined circulating MIF in SLE-PAH patients and compared them to SLE subjects without PAH but similar Systemic Lupus Erythematosus Disease Activity Index (SLEDAI) scores. There was a significant increase of circulating MIF in SLE-PAH patients' sera when compared with SLE patients without PAH or healthy donors (Fig. 2A). The correlations between circulating MIF and PASP, mPAP, or BNP in SLE-PAH patients were also analyzed by Pearson's correlation analysis. Circulating MIF levels were positively correlated with PASP ($r = 0.524$, $p = 0.045$, Fig. 2B). However, there was no correlation between MIF levels and mPAP ($r = 0.184$, $p = 0.512$, Fig. 2C); nor was correlation found between circulating MIF and BNP ($r = 0.069$, $p = 0.806$, Fig. 2D) in SLE-PAH patients.

We examined the right ventricular systolic pressure (RVSP) of 16-week-old spontaneous SLE mice (MRL/*lpr*) by right heart catheterization (RHC). High-RVSP (30.87 ± 0.56 mmHg) SLE mice served as SLE-PAH mice, and low-RVSP (22.41 ± 1.87 mmHg) SLE mice were studied as controls (Fig. 2E). The pathological characteristics of PAH were typical in high-RVSP SLE mice, with a significantly thicker media wall of distal pulmonary arteries in this group of mice (Fig. 2G). To better understand MIF expression at PA in the pathogenesis of SLE-PAH, we examined the protein expression pattern of MIF at PA from SLE-PAH mice. We observed an increase of MIF protein in pulmonary smooth muscle cells of SLE-PAH mice when compared to low-RVSP SLE mice (Fig. 2H). We also found MIF to be highly expressed in PASMC of hypoxia-induced C57BL/6J mice (Fig. 2H), which is in agreement with previously published data, and similar to that SLE-PAH mice *versus* SLE mice. Because of the variability in the development of PAH in spontaneous MRL/*lpr* SLE mice, further studies were performed with hypoxia-induced C57BL/6J mice in the following study.

3.2. MIF098 attenuated the process of hypoxia-induced pulmonary arterial hypertension of C57BL/6J mice

After 4 weeks of exposure, hypoxia-induced C57BL/6J mice showed a significant increase of RVSP, as examined by right heart catheterization (Fig. 3A). In addition, the percentage of medial wall thickness, muscularization and cardiac fibrosis were increased compared with normoxic counterparts (Fig. 3C–G). The RV / (LV + S) ratio was obviously higher in PAH mice (Fig. 3E). Notably, we observed that daily treatment with the pharmacologic MIF antagonist MIF098 (40 mg/kg) reduced RVSP, RV/(LV + S) ratio, percentage medial wall thickness, and muscularization, as well as right ventricle collagen deposition when compared with PAH mice receiving vehicle (Fig. 3A–G).

3.3. MIF098 inhibited mPASMC proliferation in in vivo and in vitro experiments

To better demonstrate the mechanism of MIF098 in ameliorating the pulmonary artery pathological process in PAH mice, lung samples from PAH, MIF098 treated-PAH, and control group mice were studied by IHC. PAH mice were found to have an increasing number of proliferative PASMCs compared with control mice. However, daily MIF098 injection reduced the percentage of proliferating cells, as stained with Ki67 (Fig. 4A), and observed by immunofluorescence. As we can see in Fig. 4C, Ki67 were downregulated by MIF098 in spite of the stimulation of PDGF-BB, a well-recognized reagent used for promoting cell proliferation in studying PAH. The effect of MIF098 on cell proliferation was proven in *in vitro* experiments. As shown in the CCK-8 assay, 20 ng/ml of PDGF-BB or 1% O_2 hypoxia significantly promoted mPASMC proliferation compared with the vehicle-treated group. However, MIF098 inhibited stimulus-induced proliferation in a concentration-dependent manner (Fig. 4E and F). Similar results were observed by EdU staining shown in Fig. 4G and I. In addition, MIF098 did not inhibit the proliferation of MIF-deficient mPASMCs, indicating that MIF098 decreased the proliferation of mPASMCs by blocking the MIF pathway (Supplementary Materials Fig. S1A). We also found that cell-cycle related proteins, such as CyclinD1, CDK4, and CDK6 were upregulated by PDGF-BB or exposed to 1% O_2 condition but decreased by 10 μM MIF098 after 48 h of treatment (Fig. 5A and C). The level of P53, P21, or P27 proteins, associated with cell-cycle arrest, were downregulated by PDGF-BB or hypoxia treatment, and the P53 and P21 protein increased when incubated together with MIF antagonist MIF098 (Fig. 5A and C).

3.4. MIF098 inhibited mPASMC migration induced by PDGF-BB

Pulmonary smooth muscle cell migration is an important feature in PAH development. As shown in Fig. 6A, more cells migrated to the lower membrane in Transwells after stimulation with PDGF-BB for 12 h compared with vehicle-treated cells. Migration was reduced by co-incubation with MIF098. The wound-healing assays supported the results of Transwell assay, MIF098 reduced the width of the scratch compared to the untreated with PDGF-BB stimulated group (Fig. 6C). We found that MIF098 did not inhibit the migration of MIF-deficient mPASMCs, indicating that MIF098 prevents mPASMC migration by blocking the MIF pathway (Supplementary Materials Fig. S1C). By western blotting, MIF098 decreased p-ERK1/2 and p-AKT expression, which was upregulated by PDGF-BB in 60 min (Fig. 6E). In addition, p-ERK1/2 and p-AKT are also important regulators in cell proliferation, indicating that MIF098 can reduce cell proliferation by inhibiting MAPK/ERK1/2 and AKT pathways.

3.5. MIF098 reduced collagen synthesis and pulmonary artery fibrosis

Aberrant deposition of fibronectin and collagen in pulmonary artery is an important characteristic of vascular remodeling in pulmonary arterial hypertension. Masson's trichrome staining showed that hypoxia-induced PAH mice had a significantly higher percentage of collagen fibers in PA than control group mice, which was attenuated by MIF098 treatment for 4 weeks (Fig. 7A). The TGFβ1/Smad2/Smad3 pathway plays a pivotal role in collagen synthesis and accumulation. Mouse TGFβ1 induced collagen synthesis or fibrosis in PASMC, as detectable by western blotting for fibronectin, collagen I, and collagen II, which were upregulated at 72 h recombinant TGFβ1 (10 ng/ml)

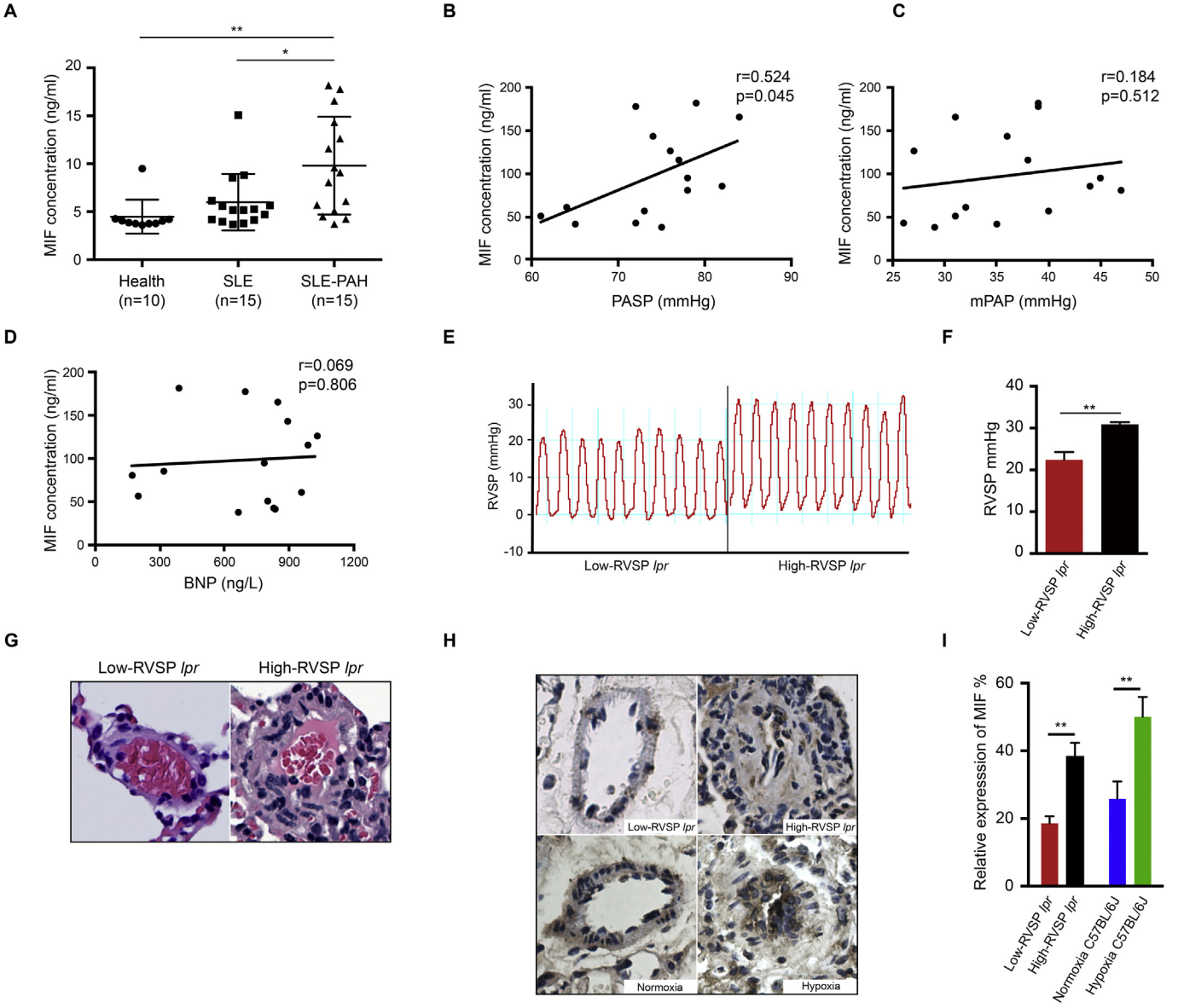

Fig. 2. MIF was elevated in SLE-PAH patients' serum and in the pulmonary arteries of high-RVSP SLE mice. (A) Circulating MIF in SLE-PAH patients (n = 15) is higher than in SLE patients (n = 15) and healthy donors (n = 10). (B)–(D) Correlation analysis between circulating MIF and PASP, mPAP, or BNP in SLE-PAH patients (n = 15). (*E*)-(G) High-RVSP SLE mice (30.87 ± 0.56 mmHg, n = 3) and low-RVSP SLE mice (22.41 ± 1.87 mmHg, n = 3) were chosen for analysis. The distal pulmonary artery wall in high-RVSP MRL/*lpr* mice is thicker than in low-RVSP *lpr* mice. (H)(I) MIF protein is highly expressed in the pulmonary arteries of high-RVSP MRL/*lpr* SLE mice, and hypoxia-induced C57BL/6J mice (n = 3). *p < 0.05, **p < 0.01.

stimulation. The production of these proteins was decreased by MIF098 treatment (Fig. 7C). MIF098 also had the effect of reducing TGFβ1-induced Smad2 and Smad3 phosphorylation (Fig. 7E). Taken together, these data support the conclusion that the MIF antagonist MIF098 reduces collagen synthesis and fibrosis in pulmonary arteries by inhibiting the TGFβ1/Smad2/3 pathway.

4. Discussion

Pulmonary arterial hypertension is a serious complication that markedly increases morbidity and mortality in patients with SLE [32], and the prognosis of SLE-associated PAH is poor compared with idiopathic PAH [4]. Conventional therapies as well as immunosuppression can reduce morbidity and prolong survival of SLE-PAH. However, the pathological process of this disease cannot be reversed. In the present study, we found that MIF expression is elevated in the serum of PAH patients with SLE compared with SLE patients without PAH, and also elevated in the pulmonary arteries of SLE-PAH mice. We also found that circulating MIF had a positive correlation with PASP in SLE-PAH patients. Pharmacologic MIF antagonism with MIF098 decreased RVSP of hypoxia-induced PAH mice and attenuated PA thickness and right ventricle hypertrophy. These effects were associated with an inhibition of PASMC proliferation, migration, and fibrosis.

There are no reliable biomarkers to indicate or evaluate SLE-associated PAH in a clinical setting. Antiphospholipid antibodies may contribute to the pathogenesis of SLE-PAH [2], and high levels of uric acid are associated with pulmonary hypertension [33]. The endothelin receptor type A (ERTA) autoantibody has also been found to be a potential biomarker of mechanistic relevance in SLE and mediate PAH development in SLE. ERTA also aggravates right ventricular hypertrophy and vascular remodeling in a monocrotaline-induced rat PAH model [34]. The role of MIF in SLE-associated PAH remains poorly understood, although the MIF/CD74 signaling axis has been implicated in contributing to a dysfunctional endothelial response in PAH (Le

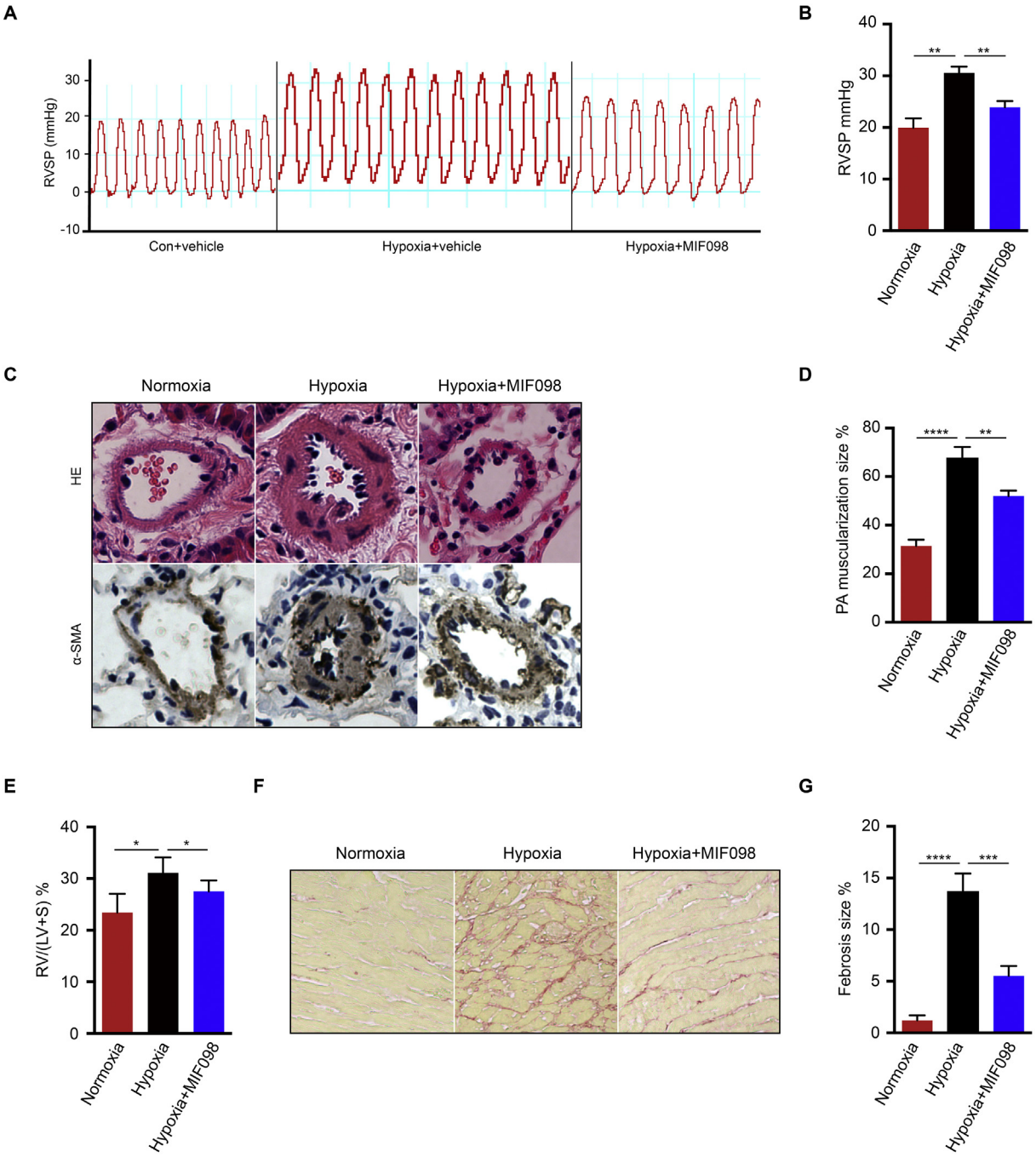

Fig. 3. MIF098 attenuates hypoxia-induced PAH and pathology in C57BL/6J mice. (A)(B) Daily treatment with MIF098 decreases RVSP of PAH mice. (C)(D) MIF098 inhibited medial wall thickness and muscularization of PAH mice. (*E*)-(G) MIF098 inhibits right ventricle hypertrophy and collagen deposition in hypoxia-induced mice. N = 4–7 in different groups. *p < 0.05, **p < 0.01, ***p < 0.001, ****p < 0.0001.

Hiress et al.). Neutralizing MIF or its receptor CD74 by antibodies or small molecule antagonists improves outcome in numerous animal models of human disease, and anti-CD74 is currently in phase II clinical testing (Wallace et al. Lupus Sci & Med). It has been well demonstrated that the circulating MIF level is positively correlated with disease activity and organ damage of SLE [35,36]. Previous studies have indicated that MIF proteins are increased in pulmonary endothelial cells and smooth muscle cells in iPAH animal models [24], and high expression MIF alleles have been linked to PAH in systemic sclerosis [37]. Right ventricle systolic pressure was downregulated, and the pathological process of PA was partially prevented when PAH model animals were treated with the first generation of MIF antagonist ISO-1 or anti-CD74 [24]. The present data indicated that the MIF level was higher in SLE-PAH patients' serum than that of healthy donors and SLE patients with similar disease severity. Circulating MIF had a positive correlation with PASP ($r = 0.524$, $p = 0.045$) in SLE-PAH patients. Additionally, in high-RVSP SLE mice, MIF protein in pulmonary arteries was also elevated compared with lower RVSP SLE mice. These results indicated that circulating MIF may have the potential to be a biomarker in SLE-associated PAH, and MIF may promote the PA pathological process of SLE-associated PAH.

Notably, we found that MIF proteins were also increased in pulmonary arteries in hypoxia-induced PAH mice, which is coincident with high-RVSP SLE mice *versus* low-RVSP SLE mice. We found that daily

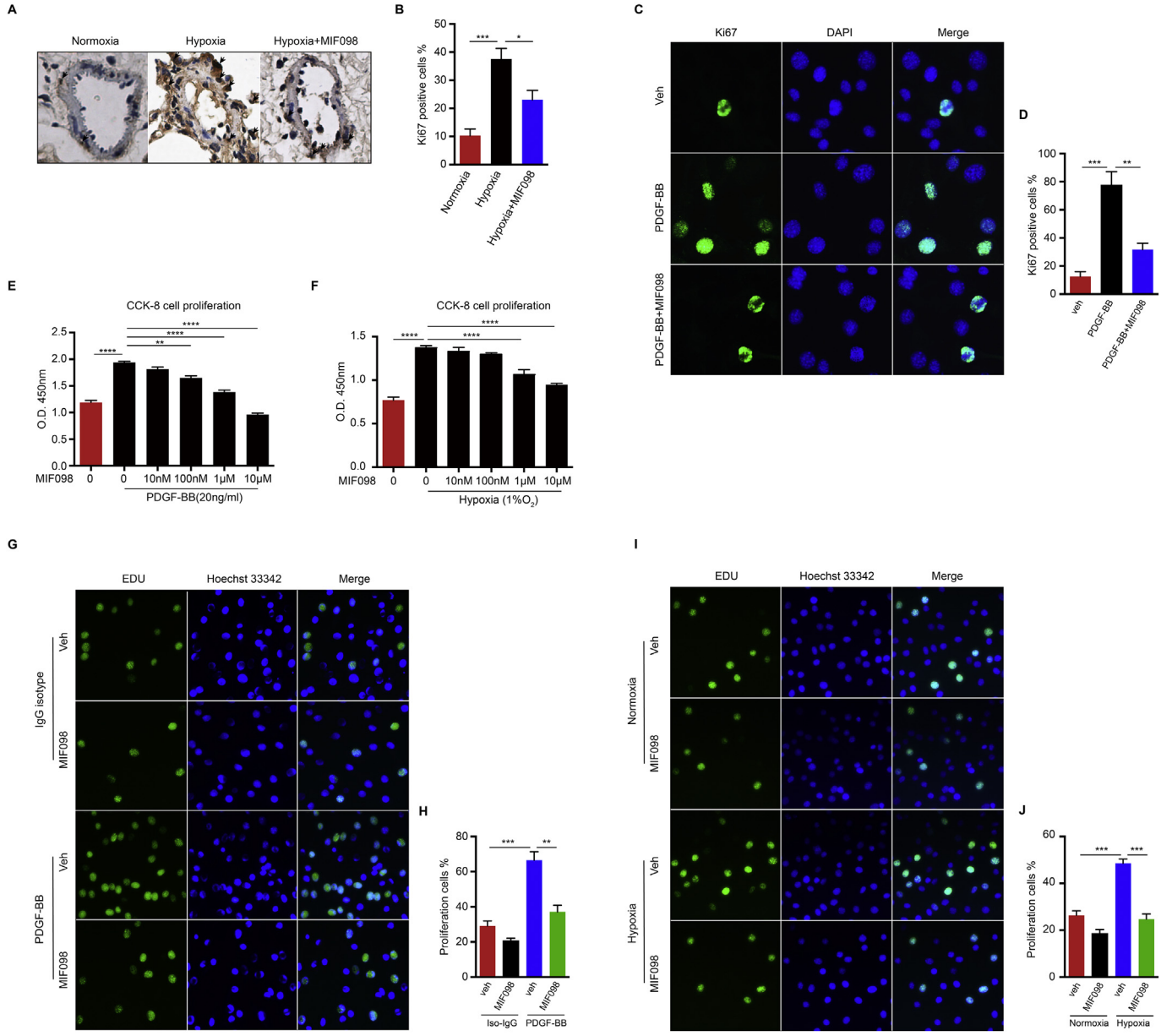

Fig. 4. MIF098 inhibits mPASMC proliferation. (A)(B) Ki67 positive smooth muscle cells are increased in PAH mice and MIF098 decreases the proportion of cells in treated PAH mice (n = 3). (C)(D) MIF098 reduced Ki67 positive mPASMCs stimulated by PDGF-BB (n = 3). (E)(F) MPASMC proliferation is decreased by MIF098 in a dose-dependent manner of both in PDGF-BB and 1% O_2 induced cell proliferation assays. $N = 4$ in each group. (G)–(J) MIF098 inhibits mPASMC proliferation induced by PDGF-BB or hypoxia in EdU assay (n = 3 in each group). *p < 0.05, **p < 0.01, ***p < 0.001, ****P < 0.0001.

intraperitoneal injection of MIF098 not only decreased RVSP, but also reduced mitigated pulmonary artery hypertrophy and right ventricular damage in PAH mice. These results were mostly benefited from the relief of pulmonary artery remodeling, generally regarded as the most important pathological mechanism in PAH, which is characterized by PASMC hyperproliferation, muscularization, and fibrosis [12]. PASMC proliferation induces distal pulmonary artery hypertrophy and narrows the pulmonary artery lumen which, together with increased collagen deposition, increases pulmonary artery stiffness. As PA pressure becomes elevated, the right ventricle becomes hypertrophic or even fails. Accordingly, therapeutic approaches should aim to reduce abnormal changes of pulmonary artery smooth muscle cells. The antiproliferative function of MIF098 to PA was evidenced by a less thick pulmonary medial layer in PAH animals, as well as the reducing expression of Ki67 in PA [38]. The result was confirmed in the PDGF-BB- or hypoxia-challenged cell experiment in CCK8, EdU, and immunofluorescence assays. It has been reported in some studies that MIF promotes cell proliferation or cell survival by activating the MAPK/ERK1/2 and AKT pathways [17,39], and cell cycle progression is considered of biological relevance in PAH [40]. Supporting our hypothesis, we found that MIF antagonist MIF098 inhibited the expression of p-ERK1/2, p-AKT, and essential cell-cycle related proteins, such as CyclinD1, CDK6, and CDK4. MIF098 also induced elevation of the P53, P21, and P27 cell-cycle arrest proteins in PASMCs.

PASMC migration also contributes to pulmonary artery remodeling in PAH [40], and inhibiting MIF using MIF098 reduced the migration of PASMCs in the challenge of PDGF-BB. Pulmonary artery fibrosis is an essential characteristic of PA in PAH, since too much collagen deposition in the medial layer is detrimental to the pulmonary artery compliance [41]. In line with the vasoconstriction theory, it was demonstrated that SLE-PAH patients have increased arterial stiffness (assessed by brachial–ankle pulse wave velocity), and this was an independent

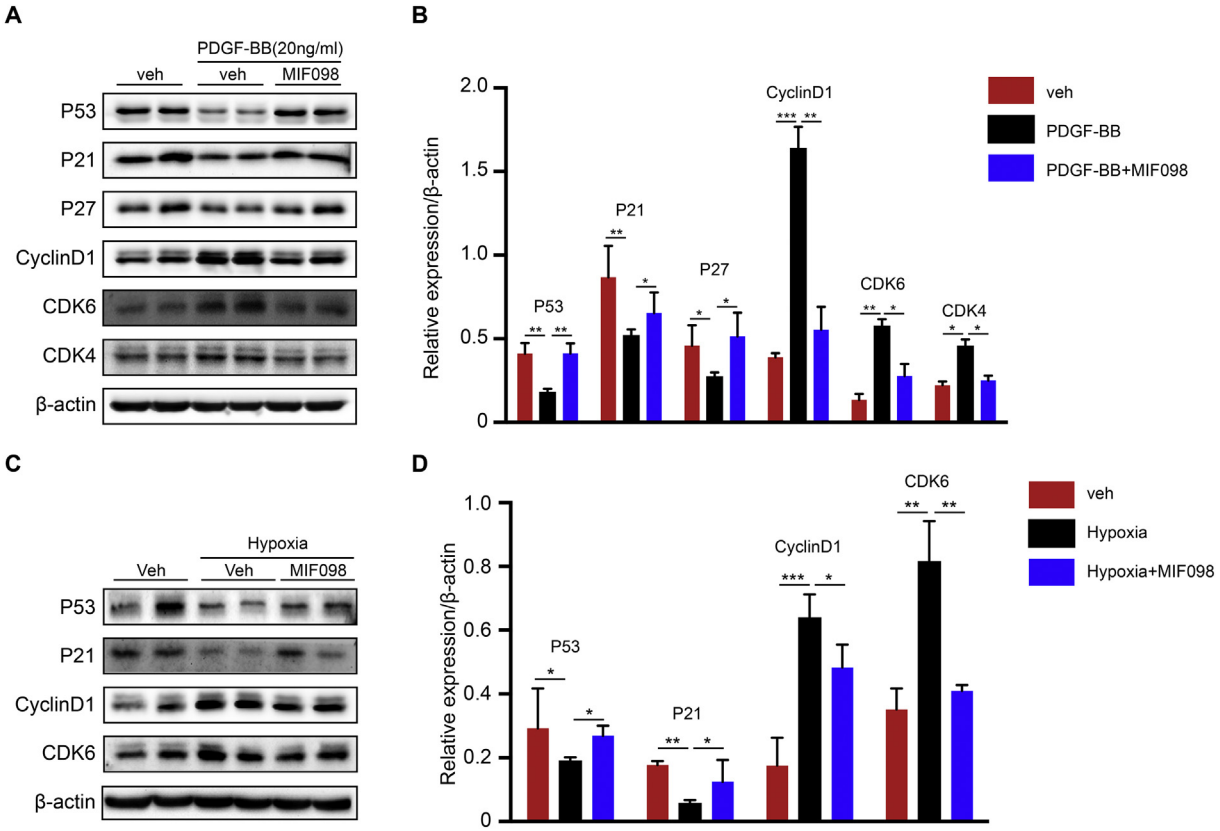

Fig. 5. Impact of MIF098 on cell-cycle related proteins in PDGF-BB- or hypoxia-stimulated cells. (A)(B) MIF098 reduces cell-cycle related protein (CyclinD1, CDK6, CDK4) and upregulated cell-cycle arrest protein (P53, P21, P27) expression after PDGF-BB stimulation (n = 4). (C)(D) MIF098 reduces CyclinD1, CDK6 and up-regulates P53 and P21 expression in hypoxic conditions (n = 4). *p < 0.05, **p < 0.01, ***p < 0.001.

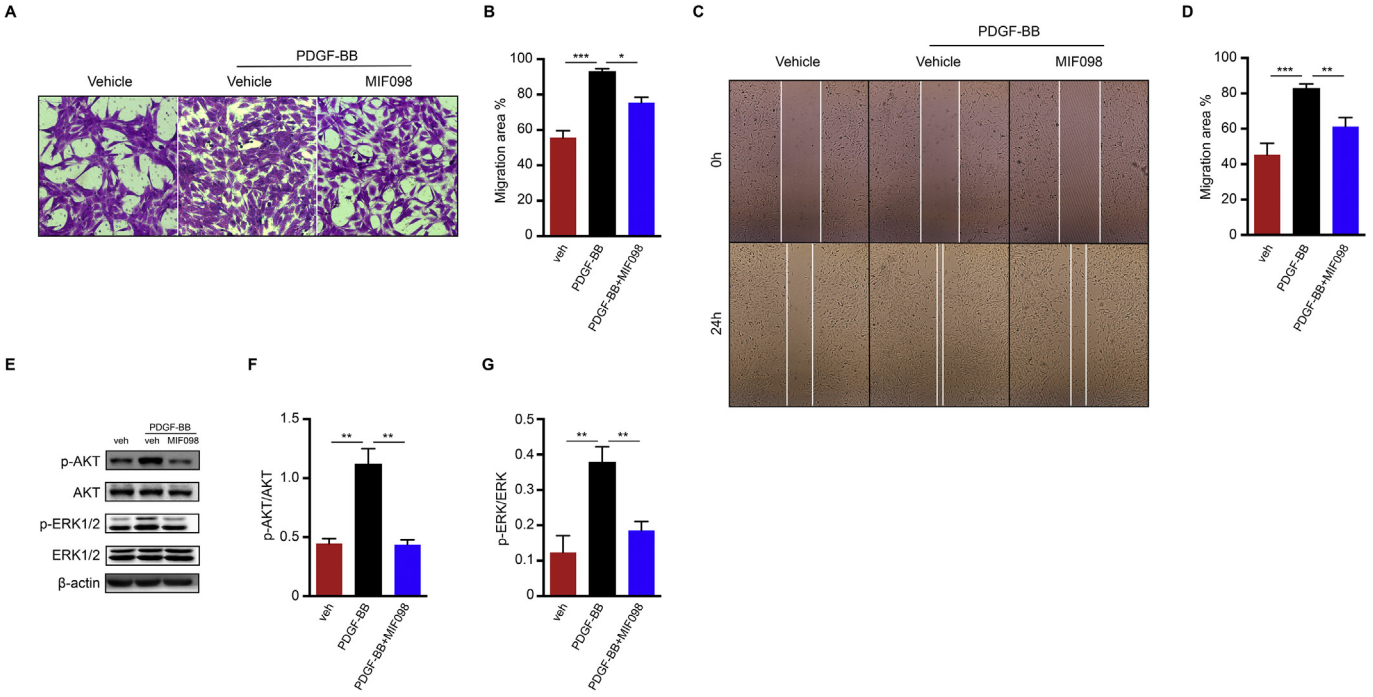

Fig. 6. MIF098 inhibits PDGF-BB-induced mPASMC migration. (A)(B) MIF098 reduces the number of migrated PASMCs in Transwell assays. N = 3 in each group. (C)(D) MIF098 decreases the healing size of mPASMCs in wound-healing assay induced by 24 h of PDGF-BB treatment (n = 3 in each group). (E)–(G) Cell migration related protein p-AKT and p-ERK1/2 are downregulated by MIF098 (n = 3). *p < 0.05, **p < 0.01, ***p < 0.001.

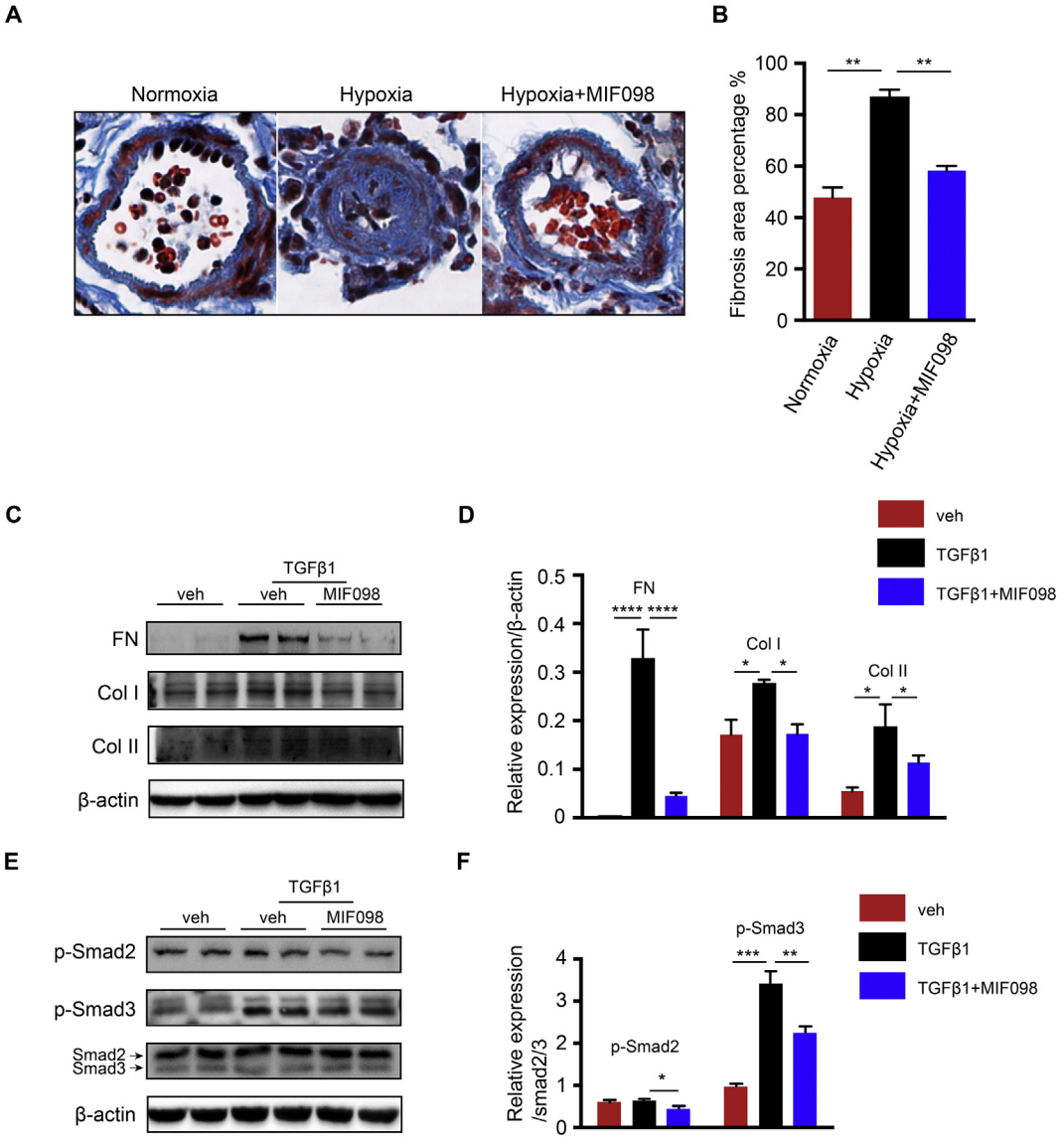

Fig. 7. MIF098 decreases fibrosis in PAH mice pulmonary artery and in TGFβ1 treated mPASMCs. (A)(B) Daily intraperitoneal injection of MIF098 attenuates PA fibrosis in PAH mice (n = 3). (C)(D) mPASMCs treated with MIF098 expressed less fibronectin (FN), collagen I (col I), and collagen II (col II) induced by TGFβ1 (n = 4). (E)(F) MIF098 decreases p-Smad2 and p-Smad3 expression in TGFβ1 stimulated mPASMCs (n = 4). *p < 0.05, **p < 0.01, ***p < 0.001, ****p < 0.0001.

predictor of PAH [42]. The function of MIF in promoting fibrosis has been reported previously [43], and the present study demonstrated that MIF expression was elevated patients' lungs with idiopathic pulmonary fibrosis [44]. Four weeks of hypoxia induced collagen synthesis in PA of PAH mice, which was reduced by daily MIF098 treatment. Our data suggested that the reduction was due to MIF inhibition of a TGFβ1/Smad2/3-dependent pathway for fibronectin and collagen I and II expression.

5. Conclusions

This study is the first to highlight MIF in SLE-associated pulmonary arterial hypertension, and it provides evidence for the efficiency of MIF098, an MIF antagonist, in preventing PAH in animal model and cell experiments. In summary, MIF098 inhibits the pathological progression of PAH, mainly by inhibiting the proliferation, migration, muscularization and fibrosis of pulmonary artery smooth muscle cells.

Supplementary data to this article can be found online at https://doi.org/10.1016/j.intimp.2019.105874.

Acknowledgments

None.

Funding

This work was supported by the National Key Research and Development Program of China (No. 2017YFC0909000) and the National Natural Science Foundation of China (No. 81974251).

Declaration of competing interest

Yale University holds patent rights to MIF098.

References

[1] L. Lisnevskaia, G. Murphy, D. Isenberg, Systemic lupus erythematosus, Lancet 384 (2014) 1878–1888, https://doi.org/10.1016/S0140-6736(14)60128-8.
[2] J. Qian, Y. Wang, C. Huang, X. Yang, J. Zhao, Q. Wang, Z. Tian, M. Li, X. Zeng, Survival and prognostic factors of systemic lupus erythematosus-associated

pulmonary arterial hypertension: a PRISMA-compliant systematic review and meta-analysis, Autoimmun. Rev. 15 (2016) 250–257, https://doi.org/10.1016/j.autrev.2015.11.012.
[3] Y. Fei, X. Shi, F. Gan, X. Li, W. Zhang, M. Li, Y. Hou, X. Zhang, Y. Zhao, X. Zeng, et al., Death causes and pathogens analysis of systemic lupus erythematosus during the past 26 years, Clin. Rheumatol. 33 (2014) 57–63, https://doi.org/10.1007/s10067-013-2383-3.
[4] R.L. Rhee, N.B. Gabler, S. Sangani, A. Praestgaard, P.A. Merkel, S.M. Kawut, Comparison of treatment response in idiopathic and connective tissue disease-associated pulmonary arterial hypertension, Am. J. Respir. Crit. Care Med. 192 (2015) 1111–1117, https://doi.org/10.1164/rccm.201507-1456OC.
[5] J. Zhao, Q. Wang, Y. Liu, Z. Tian, X. Guo, H. Wang, J. Lai, C. Huang, X. Yang, M. Li, et al., Clinical characteristics and survival of pulmonary arterial hypertension associated with three major connective tissue diseases: a cohort study in China, Int. J. Cardiol. 236 (2017) 432–437, https://doi.org/10.1016/j.ijcard.2017.01.097.
[6] S.M. Chung, C.K. Lee, E.Y. Lee, B. Yoo, S.D. Lee, H.B. Moon, Clinical aspects of pulmonary hypertension in patients with systemic lupus erythematosus and in patients with idiopathic pulmonary arterial hypertension, Clin. Rheumatol. 25 (2006) 866–872, https://doi.org/10.1007/s10067-006-0206-5.
[7] S.J. Dumas, G. Bru-Mercier, A. Courboulin, M. Quatredeniers, C. Rucker-Martin, F. Antigny, M.K. Nakhleh, B. Ranchoux, E. Gouadon, M.C. Vinhas, et al., NMDA-type glutamate receptor activation promotes vascular remodeling and pulmonary arterial hypertension, Circulation (2018), https://doi.org/10.1161/CIRCULATIONAHA.117.029930 (doi:10.1161/CIRCULATIONAHA.117.029930).
[8] K. Tselios, D.D. Gladman, M.B. Urowitz, Systemic lupus erythematosus and pulmonary arterial hypertension: links, risks, and management strategies, Open Access Rheumatol. 9 (2017) 1–9, https://doi.org/10.2147/OARRR.S123549.
[9] M. Rabinovitch, C. Guignabert, M. Humbert, M.R. Nicolls, Inflammation and immunity in the pathogenesis of pulmonary arterial hypertension, Circ. Res. 115 (2014) 165–175, https://doi.org/10.1161/CIRCRESAHA.113.301141.
[10] A. Prabu, C. Gordon, Pulmonary arterial hypertension in SLE: what do we know? Lupus 22 (2013) 1274–1285, https://doi.org/10.1177/0961203313505010.
[11] N. Nakanishi, T. Ogata, D. Naito, K. Miyagawa, T. Taniguchi, T. Hamaoka, N. Maruyama, T. Kasahara, M. Nishi, S. Matoba, et al., MURC deficiency in smooth muscle attenuates pulmonary hypertension, Nat. Commun. 7 (2016) 12417, , https://doi.org/10.1038/ncomms12417.
[12] L. Jiang, H. Konishi, F. Nurwidya, K. Satoh, F. Takahashi, H. Ebinuma, K. Fujimura, K. Takasu, M. Jiang, H. Shimokawa, et al., Deletion of LR11 attenuates hypoxia-induced pulmonary arterial smooth muscle cell proliferation with medial thickening in mice, Arterioscler. Thromb. Vasc. Biol. 36 (2016) 1972–1979, https://doi.org/10.1161/ATVBAHA.116.307900.
[13] T. Lang, J.P.W. Lee, K. Elgass, A.A. Pinar, M.D. Tate, E.H. Aitken, H. Fan, S.J. Creed, N.S. Deen, D.A.K. Traore, et al., Macrophage migration inhibitory factor is required for NLRP3 inflammasome activation, Nat. Commun. 9 (2018) 2223, https://doi.org/10.1038/s41467-018-04581-2.
[14] Z. Cournia, L. Leng, S. Gandavadi, X. Du, R. Bucala, W.L. Jorgensen, Discovery of human macrophage migration inhibitory factor (MIF)-CD74 antagonists via virtual screening, J. Med. Chem. 52 (2009) 416–424, https://doi.org/10.1021/jm801100v.
[15] L.M. Marsh, L. Cakarova, G. Kwapiszewska, W. von Wulffen, S. Herold, W. Seeger, J. Lohmeyer, Surface expression of CD74 by type II alveolar epithelial cells: a potential mechanism for macrophage migration inhibitory factor-induced epithelial repair, Am. J. Physiol. Lung Cell. Mol. Physiol. 296 (2009) L442–L452, https://doi.org/10.1152/ajplung.00525.2007.
[16] B. Schroder, The multifaceted roles of the invariant chain CD74–more than just a chaperone, Biochim. Biophys. Acta 1863 (2016) 1269–1281, https://doi.org/10.1016/j.bbamcr.2016.03.026.
[17] H. Lue, A. Kapurniotu, G. Fingerle-Rowson, T. Roger, L. Leng, M. Thiele, T. Calandra, R. Bucala, J. Bernhagen, Rapid and transient activation of the ERK MAPK signalling pathway by macrophage migration inhibitory factor (MIF) and dependence on JAB1/CSN5 and Src kinase activity, Cell. Signal. 18 (2006) 688–703, https://doi.org/10.1016/j.cellsig.2005.06.013.
[18] R.A. Mitchell, H. Liao, J. Chesney, G. Fingerle-Rowson, J. Baugh, J. David, R. Bucala, Macrophage migration inhibitory factor (MIF) sustains macrophage proinflammatory function by inhibiting p53: regulatory role in the innate immune response, Proc. Natl. Acad. Sci. U. S. A. 99 (2002) 345–350, https://doi.org/10.1073/pnas.012511599.
[19] E.F. Morand, M. Leech, J. Bernhagen, MIF: a new cytokine link between rheumatoid arthritis and atherosclerosis, Nat. Rev. Drug Discov. 5 (2006) 399–410, https://doi.org/10.1038/nrd2029.
[20] C. Corallo, L. Paulesu, M. Cutolo, F. Ietta, C. Carotenuto, C. Mannelli, R. Romagnoli, R. Nuti, N. Giordano, Serum levels, tissue expression and cellular secretion of macrophage migration inhibitory factor in limited and diffuse systemic sclerosis, Clin. Exp. Rheumatol. 33 (2015) S98–105.
[21] K. Stefanantoni, I. Sciarra, M. Vasile, R. Badagliacca, R. Poscia, M. Pendolino, C. Alessandri, C.D. Vizza, G. Valesini, V. Riccieri, Elevated serum levels of macrophage migration inhibitory factor and stem cell growth factor beta in patients with idiopathic and systemic sclerosis associated pulmonary arterial hypertension, Reumatismo 66 (2015) 270–276, https://doi.org/10.4081/reumatismo.2014.774.
[22] A. Sparkes, P. De Baetselier, L. Brys, I. Cabrito, Y.G. Sterckx, S. Schoonooghe, S. Muyldermans, G. Raes, R. Bucala, P. Vanlandschoot, et al., Novel half-life extended anti-MIF nanobodies protect against endotoxic shock, FASEB J. 32 (2018) 3411–3422, https://doi.org/10.1096/fj.201701189R.
[23] B. Zhang, M. Shen, M. Xu, L.L. Liu, Y. Luo, D.Q. Xu, Y.X. Wang, M.L. Liu, Y. Liu, H.Y. Dong, et al., Role of macrophage migration inhibitory factor in the proliferation of smooth muscle cell in pulmonary hypertension, Mediat. Inflamm. 2012 (2012) 840737, , https://doi.org/10.1155/2012/840737.
[24] M. Le Hiress, L. Tu, N. Ricard, C. Phan, R. Thuillet, E. Fadel, P. Dorfmuller, D. Montani, F. de Man, M. Humbert, et al., Proinflammatory signature of the dysfunctional endothelium in pulmonary hypertension. Role of the macrophage migration inhibitory factor/CD74 complex, Am. J. Respir. Crit. Care Med. 192 (2015) 983–997, https://doi.org/10.1164/rccm.201402-0322OC.
[25] H.M. DuBrock, J.M. Rodriguez-Lopez, B.L. LeVarge, M.P. Curry, P.A. VanderLaan, Z.K. Zsengeller, E. Pernicone, I.R. Preston, P.B. Yu, I. Nikolic, et al., Macrophage migration inhibitory factor as a novel biomarker of portopulmonary hypertension, Pulm Circ. 6 (2016) 498–507, https://doi.org/10.1086/688489.
[26] Y. Zhang, A. Talwar, D. Tsang, A. Bruchfeld, A. Sadoughi, M. Hu, K. Omonuwa, K.F. Cheng, Y. Al-Abed, E.J. Miller, Macrophage migration inhibitory factor mediates hypoxia-induced pulmonary hypertension, Mol. Med. 18 (2012) 215–223, https://doi.org/10.2119/molmed.2011.00094.
[27] M.S. Shin, Y. Kang, E.R. Wahl, H.J. Park, R. Lazova, L. Leng, M. Mamula, S. Krishnaswamy, R. Bucala, I. Kang, Macrophage migration inhibitory factor regulates U1 small nuclear RNP immune complex-mediated activation of the NLRP3 inflammasome, Arthritis Rheumatol. 71 (2019) 109–120, https://doi.org/10.1002/art.40672.
[28] S.A. Yoo, L. Leng, B.J. Kim, X. Du, P.V. Tilstam, K.H. Kim, J.S. Kong, H.J. Yoon, A. Liu, T. Wang, et al., MIF allele-dependent regulation of the MIF coreceptor CD44 and role in rheumatoid arthritis, Proc. Natl. Acad. Sci. U. S. A. 113 (2016) E7917–E7926, https://doi.org/10.1073/pnas.1612717113.
[29] A.A. Hare, L. Leng, S. Gandavadi, X. Du, Z. Cournia, R. Bucala, W.L. Jorgensen, Optimization of N-benzyl-benzoxazol-2-ones as receptor antagonists of macrophage migration inhibitory factor (MIF), Bioorg. Med. Chem. Lett. 20 (2010) 5811–5814, https://doi.org/10.1016/j.bmcl.2010.07.129.
[30] M.C. Hochberg, Updating the American College of Rheumatology revised criteria for the classification of systemic lupus erythematosus, Arthritis Rheum. 40 (1997) 1725, https://doi.org/10.1002/1529-0131(199709)40:9<1725::AID-ART29>3.0.CO;2-Y.
[31] L. Xu, Y. Su, Y. Zhao, X. Sheng, R. Tong, X. Ying, L. Gao, Q. Ji, Y. Gao, Y. Yan, et al., Melatonin differentially regulates pathological and physiological cardiac hypertrophy: Crucial role of circadian nuclear receptor RORalpha signaling, J. Pineal Res. 67 (2019) e12579 https://doi.org/10.1111/jpi.12579.
[32] J.S. Kim, D. Kim, Y.B. Joo, S. Won, J. Lee, J. Shin, S.C. Bae, Factors associated with development and mortality of pulmonary hypertension in systemic lupus erythematosus patients, Lupus 27 (2018) 1769–1777, https://doi.org/10.1177/0961203318788163.
[33] K.J. Kim, I.W. Baek, Y.J. Park, C.H. Yoon, W.U. Kim, C.S. Cho, High levels of uric acid in systemic lupus erythematosus is associated with pulmonary hypertension, Int. J. Rheum. Dis. 18 (2015) 524–532, https://doi.org/10.1111/1756-185X.12262.
[34] L. Guo, M. Li, Y. Chen, Q. Wang, Z. Tian, S. Pan, X. Zeng, S. Ye, Anti-endothelin receptor type a autoantibodies in systemic lupus erythematosus-associated pulmonary arterial hypertension, Arthritis Rheumatol. 67 (2015) 2394–2402, https://doi.org/10.1002/art.39212.
[35] K.L. Connelly, R. Kandane-Rathnayake, A. Hoi, M. Nikpour, E.F. Morand, Association of MIF, but not type I interferon-induced chemokines, with increased disease activity in Asian patients with systemic lupus erythematosus, Sci. Rep. 6 (2016) 29909, , https://doi.org/10.1038/srep29909.
[36] A. Foote, E.M. Briganti, Y. Kipen, L. Santos, M. Leech, E.F. Morand, Macrophage migration inhibitory factor in systemic lupus erythematosus, J. Rheumatol. 31 (2004) 268–273.
[37] L. Bossini-Castillo, D. Campillo-Davo, E. Lopez-Isac, F.D. Carmona, C.P. Simeon, P. Carreira, J.L. Callejas-Rubio, I. Castellvi, A. Fernandez-Nebro, L. Rodriguez-Rodriguez, et al., An MIF promoter polymorphism is associated with susceptibility to pulmonary arterial hypertension in diffuse cutaneous systemic sclerosis, J. Rheumatol. 44 (2017) 1453–1457, https://doi.org/10.3899/jrheum.161369.
[38] Y. Yue, Z. Zhang, L. Zhang, S. Chen, Y. Guo, Y. Hong, miR-143 and miR-145 promote hypoxia-induced proliferation and migration of pulmonary arterial smooth muscle cells through regulating ABCA1 expression, Cardiovasc. Pathol. 37 (2018) 15–25, https://doi.org/10.1016/j.carpath.2018.08.003.
[39] M. Sauler, Y. Zhang, J.N. Min, L. Leng, P. Shan, S. Roberts, W.L. Jorgensen, R. Bucala, P.J. Lee, Endothelial CD74 mediates macrophage migration inhibitory factor protection in hyperoxic lung injury, FASEB J. 29 (2015) 1940–1949, https://doi.org/10.1096/fj.14-260299.
[40] Z. Qian, Y. Li, H. Yang, J. Chen, X. Li, D. Gou, PDGFBB promotes proliferation and migration via regulating miR-1181/STAT3 axis in human pulmonary arterial smooth muscle cells, Am. J. Physiol. Lung Cell. Mol. Physiol. (2018), https://doi.org/10.1152/ajplung.00224.2018 (doi:10.1152/ajplung.00224.2018).
[41] D. Jia, Y. He, Q. Zhu, H. Liu, C. Zuo, G. Chen, Y. Yu, A. Lu, RAGE-mediated extracellular matrix proteins accumulation exacerbates HySu-induced pulmonary hypertension, Cardiovasc. Res. 113 (2017) 586–597, https://doi.org/10.1093/cvr/cvx051.
[42] J.H. Lee, K. Im Cho, Arterial stiffness, antiphospholipid antibodies, and pulmonary arterial hypertension in systemic lupus erythematosus, J. Cardiol. 64 (2014) 450–455, https://doi.org/10.1016/j.jjcc.2014.02.030.
[43] M.A. Barnes, M.R. McMullen, S. Roychowdhury, N.Z. Madhun, K. Niese, M.A. Olman, A.B. Stavitsky, R. Bucala, L.E. Nagy, Macrophage migration inhibitory factor is required for recruitment of scar-associated macrophages during liver fibrosis, J. Leukoc. Biol. 97 (2015) 161–169, https://doi.org/10.1189/jlb.3A0614-280R.
[44] C. Olivieri, E. Bargagli, S. Inghilleri, I. Campo, M. Cintorino, P. Rottoli, Macrophage migration inhibitory factor in lung tissue of idiopathic pulmonary fibrosis patients, Exp. Lung Res. 42 (2016) 263–266, https://doi.org/10.1080/01902148.2016.1199744.